FEASIBILITY STUDY OF A DIGITAL HYDRAULIC WINCH DRIVE SYSTEM

Sondre Nordås, Morten Kjeld Ebbesen, Torben Ole Andersen*
University of Agder
Jon Lilletunsvei 9, Grimstad 4879, Norway
*Aalborg University
*Pontoppidanstraede 101, 9220 Aalborg East, Denmark
E-mail: sondre.nordas@uia.no, morten.k.ebbesen@uia.no, toa@et.aau.dk
Phone: +47 3723 3198

ABSTRACT

The offshore oil and gas industry has traditionally used hydraulically driven applications. Hydraulic systems are known to suffer from relatively low efficiency. Due to environmental issues, more efficient systems are now required. Today, the offshore oil and gas industry is experiencing a shift in driveline systems; high efficient electric motors tend to replace low efficient hydraulic systems. In addition to the electric motors, a new alternative to the conventional hydraulic system is digital hydraulic machines. This paper investigates the feasibility of using a digital hydraulic winch drive system and presents a new digital hydraulic winch drive control system. The simulated system is based on a 20000 *kg* hydraulic offshore auxiliary winch with a drum capacity of 3600 *m* of wire. The digital hydraulic winch drive system is a closed-circuit system with one high-speed digital pump and one low-speed high-torque digital motor. One of the biggest challenges in digital hydraulic pump/motor technology is the fast switching on/off valves. The valves must have high durability, low power consumption, zero leakage and low response time. The on/off valves in this study are modeled with an ideal behavior. The simulation results show that the payload follows the reference trajectory when using a digital hydraulic winch drive system for a wide range of loads and speeds.

KEYWORDS: Digital hydraulic pump/motor, hydraulic offshore winch, simulation

1 INTRODUCTION

Digital hydraulic pumps and motors differ from traditional variable displacement machines (typically piston type machines) in the way they achieve variable displacement. Traditionally variable displacement machines change displacement by changing the piston stroke. Hence, every cylinder is pressurized and depressurized during one shaft revolution. Leakage losses, friction losses and compressibility losses are therefore almost constant independent of displacement which results in poor efficiency at partial displacement. In digital hydraulic machines, two fast switching on/off valves are connected to

every single cylinder, one between the high-pressure manifold and the cylinder, and the other one between the cylinder and the low-pressure manifold. By controlling the on/off valves, every cylinder can be individually controlled. One cylinder can be active (operate in motor mode or pump mode) or be idling. In idle mode, the low-pressure valve is kept open during the entire shaft revolution. The displacement of the pump or motor is changed by changing the ratio of active cylinders and idling cylinders. During idling, the cylinder pressure is kept low resulting in a minimum of losses and high component efficiency even at partial displacement.

Digital hydraulic machines have earlier been proposed to be used in hydrostatic transmissions for large wind turbines. The company Artemis Intelligent Power (Artemis IP) is the leading pioneer in digital displacement technology and develops systems with digital displacement technology for a wide range of applications. In 2010 Mitsubishi Heavy Industries started developing a 7 MW wind turbine with a hydrostatic transmission using the digital displacement technology from Artemis IP. This digital hydraulic transmission consists of a 7 MW digital pump and two 3.5 MW digital motors driving two generators [1]. The total efficiency of the transmission is approximately 94%, 98% for the digital pump and 96% for the digital motors [2]. Artemis IP has with the hydrostatic transmission shown that digital hydraulic machines have the potential of converting slow rotational movement with high torque into high and steady rotational speed appropriate for generating electricity. However, is it possible to use digital hydraulic machines to transform high constant speed with low torque into variable high torque and low-speed movement?

The offshore oil and gas industry has several high torque low-speed applications, for example, mud pumps, top drives, drawworks, and winches. In the offshore oil and gas industry, winches are used in big cranes for heavy lifting operations but can also be used for smaller lifting operations on the drill floor and at the moon pool. One drilling unit can have several deck cranes for deck-to-deck lifting as well as loading and unloading of supply vessels and subsea lifting operations. Deck cranes come in different types and size, and at the moment the biggest cranes can have a safe working load up to 800 tons. Cranes on floating drilling units are often equipped with active heave compensation systems to compensate for the vertical motion caused by the waves when landing loads at the seabed. The hydraulic system on huge winches is often a closed circuit system with a variable displacement pump providing fluid to one or several variable displacement high-speed motors. A gearbox is connected between the motors and the winch drum. This system suffers from poor efficiency, especially when handling low loads. The present work investigates the feasibility of using digital hydraulic machines in a closed circuit system where the digital motor is directly connected to the drum.

2 SIMULATION MODEL

The simulated system is based on a 20000 kg hydraulic offshore auxiliary winch with a capacity of 3600 m of wire. The digital hydraulic winch drive system consists of a digital hydraulic pump (DHP), a digital hydraulic motor (DHM), and two gas accumulators connected in a closed circuit system, as shown in Figure 1. The DHP is driven by an electrical motor running at a constant speed of 1800 rpm. The DHM is directly connected to the winch drum without any gear box. The two gas accumulators are used to smooth out pressure and flow peaks in line A and B.

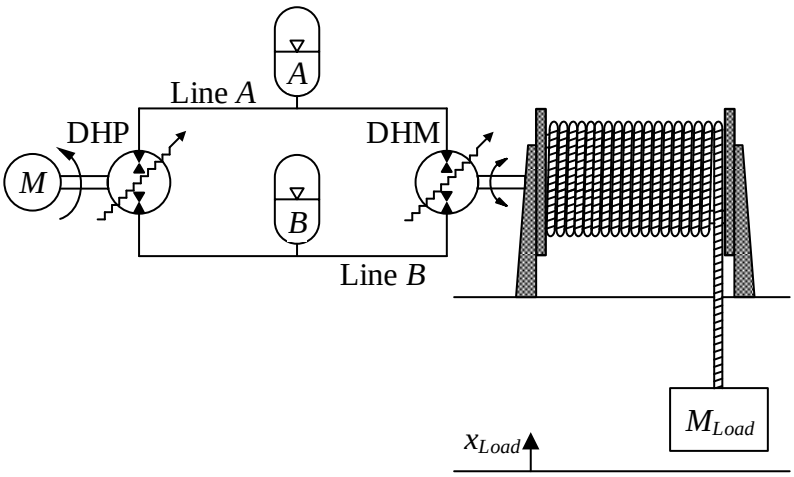

Figure 1: Simulated winch system

2.1 Modeling of the Mechanical System

The mechanical system consists of the load, wire and the drum. All relevant winch parameters are shown in Figure 2.

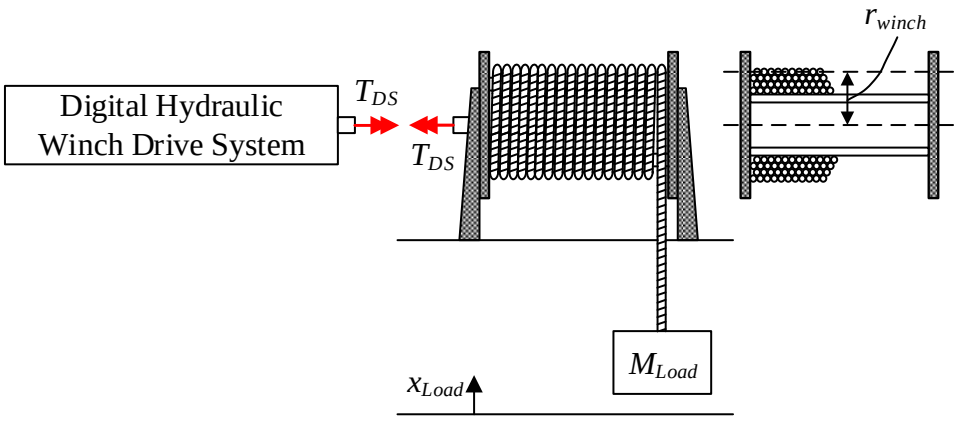

Figure 2: Mechanical system

Assumptions made for the mechanical system:

- Winch has constant inertia. The winch inertia includes the inertia of the drum and the inertia of 3600 m of wire wound onto the drum.
- Radius of the winch, r_{winch}, is constant
- No friction
- No elasticity in wire

It is assumed that the winch has a constant inertia because no simulation hoists or lowers the payload more than 10 m, which is very small compared to the total wire length. The radius is also assumed to be constant because only the outer wire layer is used. The equation of motion for the winch drum is shown in Eq. 1.

$$\ddot{\theta}_{drum} = \frac{T_{DS} - M_{Load} \cdot g \cdot r_{winch}}{J_{eff}} \tag{1}$$

where T_{DS} is the torque from the drive system acting on the drum, M_{Load} is the mass of the payload, g is the acceleration of gravity, r_{winch} is the radius of the outer winch layer, and J_{eff} is the effective mass moment of inertia. The effective mass moment of inertia includes the inertia of the payload, wire, drum and the DHM and is calculated as shown below in Eq. 2.

$$J_{eff} = M_{Load} \cdot r_{winch}^2 + J_{winch} + J_{DS} \tag{2}$$

where J_{winch} includes the inertia of the drum and the wire wound on the drum and J_{DS} is the inertia of the DHM. The drive torque, T_{DS}, is given in the following section.

2.2 Modeling of the Digital Hydraulic Winch Drive System

The digital hydraulic winch drive system is a closed circuit system, see Figure 3. The DHP and the DHM are two radial piston units with respectively 9 and 42 cylinders. Each one of the lines A and B are connected to an accumulator. The accumulator purpose is to smooth out flow and pressure peaks in the closed circuit system.

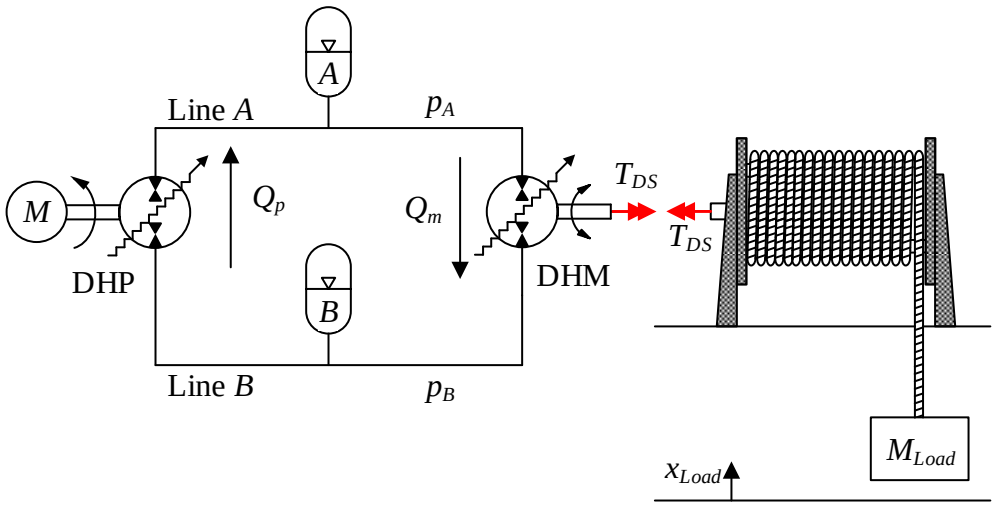

Figure 3: Digital hydraulic winch drive system

2.2.1 Modeling of the Digital Hydraulic Pump and Motor

It is assumed that the cylinder configuration is the same for both the DHP and the DHM. For simplicity, only calculations for one of the pistons in the DHM are shown in this section, but the same method is used for all of the pistons, both for the DHM and the DHP. The on/off valves are assumed to be leak free and the DHP and DHM models do not include any friction or leakage.

Figure 4 shows the cylinder configuration of one cylinder, note that a more complex cylinder configuration may also be used. The continuity equation is used to calculate the pressure gradient in the cylinder as shown in Eq. 3.

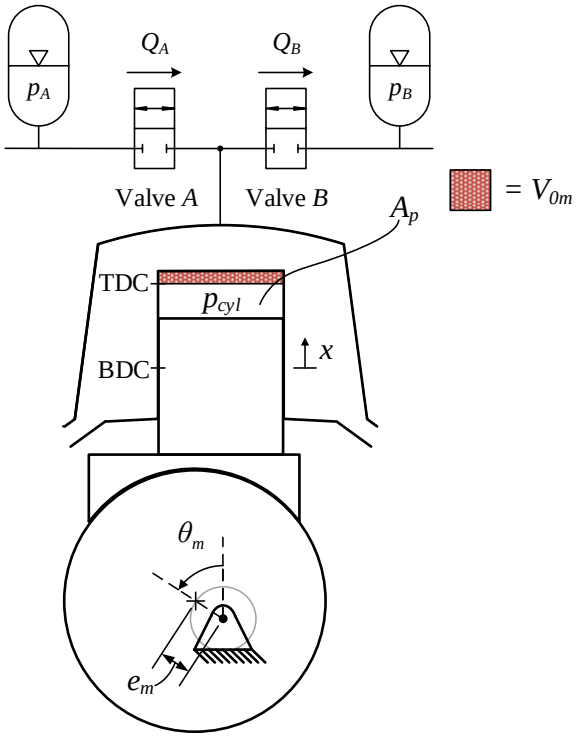

Figure 4: Cylinder configuration of one cylinder with $\theta_m = \pi/4$

$$\dot{p}_{cyl} = \frac{\beta}{V_{cyl}} \cdot \left(Q_A - Q_B - \dot{V}_{cyl}\right) \tag{3}$$

where β is the effective bulk modulus, V_{cyl} is the cylinder volume, Q_A and Q_B are the flows through valve A and B, and $\dot{V}_{cyl}$ is the rate of change in cylinder volume and is positive if the volume is expanding. The cylinder volume is calculated as shown in Eq. 4 and the rate of change in cylinder volume is calculated as shown in Eq. 5.

$$V_{cyl} = V_{0m} + \frac{V_{dm}}{2} \cdot (1 - \cos(\theta_m)) \tag{4}$$

$$\dot{V}_{cyl} = \frac{V_{dm}}{2} \cdot \sin(\theta_m) \cdot \dot{\theta}_m \tag{5}$$

where V_{0m} is the dead volume in the cylinder and V_{dm} is the piston discharge volume. The flow through the on/off valves, Q_A and Q_B, are calculate by Eq. 6 and Eq. 7 respectively.

$$Q_A = \frac{u_A}{k_f} \cdot \sqrt{p_A - p_{cyl}} \cdot sign(p_A - p_{cyl}) \tag{6}$$

$$Q_B = \frac{u_B}{k_f} \cdot \sqrt{p_{cyl} - p_B} \cdot sign(p_{cyl} - p_B) \tag{7}$$

where k_f is the flow coefficient of the valves, and u_A and u_B are the opening ratios of the valves ranging from 0 to 1, where 0 is fully closed and 1 is fully open. Valve A and B have the same flow coefficient and the same dynamic response. The dynamic response is described by the second order system shown in Eq. 8.

$$\ddot{u} = u_{con} \cdot \omega^2 - u \cdot \omega^2 - 2 \cdot \zeta \cdot \omega \cdot \dot{u} \tag{8}$$

where u_{con} is the control signal, ζ is the damping ratio and ω is the natural frequency. The control signal is either 0 or 1. The torque contribution from one cylinder is calculated as shown in Equation 9

$$T_{cyl} = p_{cyl} \cdot A_p \cdot e_m \cdot \sin(\theta_m) \tag{9}$$

Finally, the total motor torque and the flow in and out of the DHM are calculated as the sum of the contribution from all pistons, as shown below in Eq. 10, 11 and 12 respectively.

$$T_{DS} = \sum_{i=1}^{42} T_{cyl,i} \tag{10}$$

$$Q_{inm} = \sum_{i=1}^{42} Q_{A,i} \tag{11}$$

$$Q_{outm} = \sum_{i=1}^{42} Q_{B,i} \tag{12}$$

2.2.2 Valve Control Strategy in Motor Mode

The timing of the valve actuation is important to achieve high efficiency and low pressure and flow peaks. The activation angles when operating in motor mode are shown in the simplified control sequence illustration in Fig. 5. θ_{Ao} and θ_{Ac} are respectively the opening and closing angles for valve A, θ_{Bo} and θ_{Bc} are respectively the opening and closing angles for valve B and θ_{mcm} is the mode choice angel for the motor and is the angle where it is decided if the motor shall run in motor or idle mode.

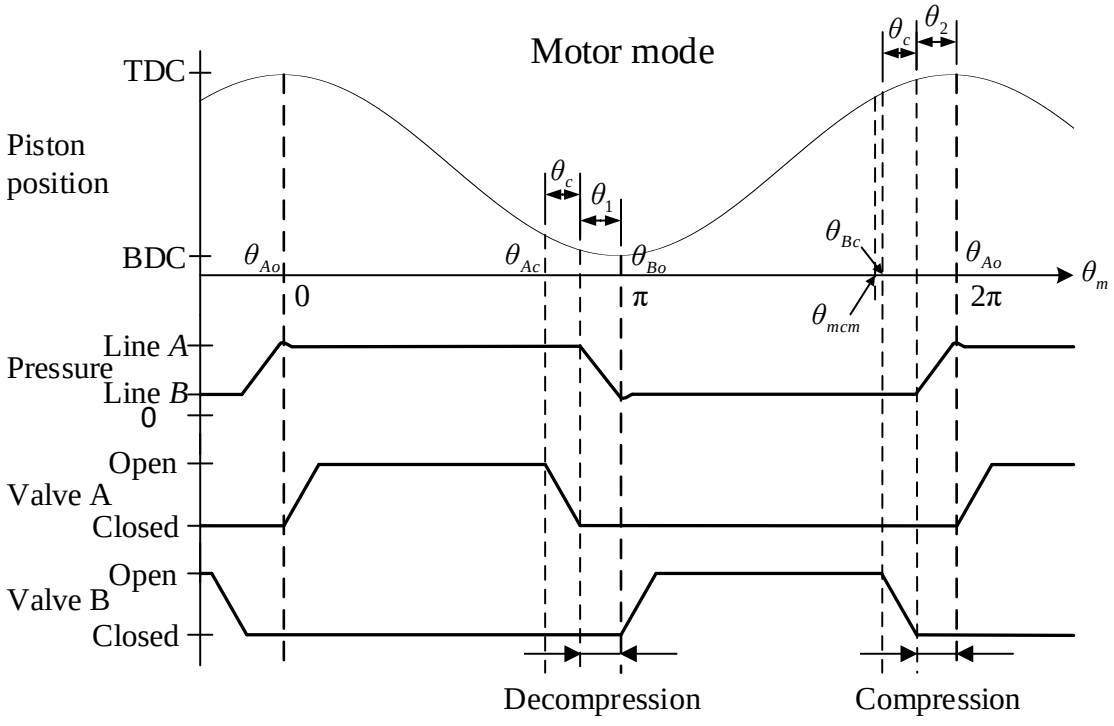

Figure 5: Control sequence motor mode

The opening angle and closing angle for valve A and B are calculated as shown in Eq. 13..16.

$$\theta_{Ao} = 0 \tag{13}$$
$$\theta_{Ac} = \pi - \theta_1 - \theta_c \tag{14}$$
$$\theta_{Bo} = \pi \tag{15}$$
$$\theta_{Bc} = 2 \cdot \pi - \theta_2 - \theta_c \tag{16}$$

where θ_1 is the angle the motor have to rotate to decompress the cylinder fluid from high-pressure level down to low-pressure level when the piston is close to and moving towards BDC. θ_2 is the angle the motor have to rotate to compress the cylinder fluid from low-pressure level up to high-pressure level when the piston is close to and moving towards TDC and θ_c is the angle the motor rotates while closing or opening the valve. The closing angle, θ_c, is given by Eq. 17

$$\theta_c = \dot{\theta}_m \cdot t_s \tag{17}$$

where $\dot{\theta}_m$ is the motor speed and t_s is the valve traveling time.

The change in cylinder volume to compress or decompress the cylinder fluid is calculated based on the continuity equation shown in Eq. 3.

$$\begin{aligned} \Delta p &= \frac{\beta}{V_{cyl}} \cdot \Delta V \\ &\Downarrow \\ \Delta V &= \frac{V_{cyl} \cdot \Delta p}{\beta} \end{aligned} \tag{18}$$

When calculating θ_1, the piston is close to BDC and the cylinder volume, V_{cyl} is assumed to be $V_{cyl1} = V_0 + V_{dm}$, and when calculating θ_2 the piston is close to TDC and the cylinder volume is assumed to be $V_{cyl2} = V_0$. The change in cylinder volume to compress and decompress the cylinder fluid is calculated as:

$$\Delta V_1 = \frac{V_{cyl1} \cdot (p_A - p_B)}{\beta} \tag{19}$$
$$\Delta V_2 = \frac{V_{cyl2} \cdot (p_A - p_B)}{\beta} \tag{20}$$

Knowing the needed change in volume, θ_1 and θ_2 are calculated as shown below.

$$\theta_1 = \cos^{-1}\left(1 - \frac{\Delta V_1 \cdot 2}{V_{dm}}\right) \tag{21}$$
$$\theta_2 = \cos^{-1}\left(1 - \frac{\Delta V_2 \cdot 2}{V_{dm}}\right) \tag{22}$$

2.2.3 Valve Control Strategy in Pump Mode

The opening and closing angles for valve A and B in pump mode and the mode choice angle for the pump, θ_{mcp}, are illustrated in Fig. 6. The opening and closing angles for the valves are calculated as shown in Eq. 23..26.

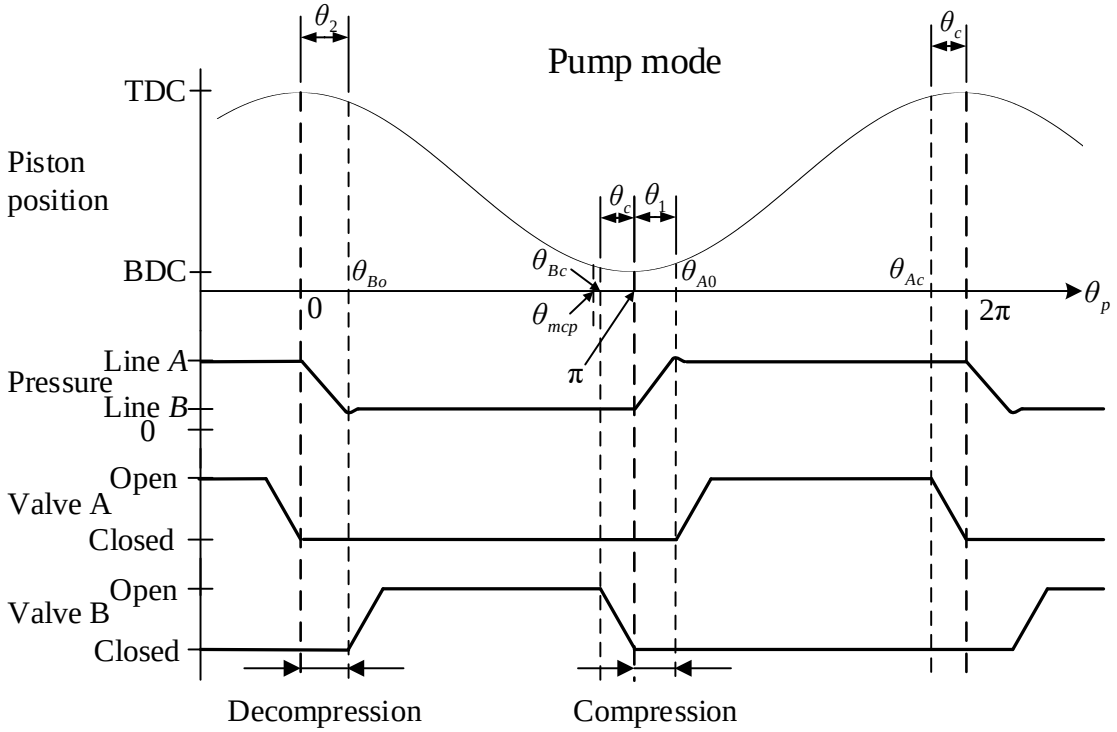

Figure 6: Control sequence pump mode

$$\theta_{Ao} = \pi + \theta_1 \tag{23}$$
$$\theta_{Ac} = 2 \cdot \pi - \theta_c \tag{24}$$
$$\theta_{Bo} = \theta_2 \tag{25}$$
$$\theta_{Bc} = \pi - \theta_c \tag{26}$$

where θ_c, θ_1 and θ_2 are calculated as shown in Eq. 17, 21 and 22 respectively.

2.2.4 Pressure dynamics in line *A* and line *B*

For simplicity, only the calculation for the pressure dynamics in line A is shown, but the pressure dynamics in line B is calculated in the same manner. The pressure gradient in line A is calculated as shown in Eq. 27

$$\dot{p}_A = \frac{\beta}{V_A} \cdot (Q_{outp} - Q_{inm} - \dot{V}_{accA}) \tag{27}$$

where V_A is the volume in line A and accumulator A, Q_{outp} is the flow out of the pump, Q_{inm} is the flow into the motor and $\dot{V}_{accA}$ is the rate of changing of accumulator volume.

$\dot{V}_{accA}$ is positive if the volume is expanding and is calculated as shown below in Eq. 28

$$\dot{V}_{accA} = \dot{p}_A \cdot \frac{V_{accAg}}{n_{accA} \cdot p_A} \tag{28}$$

where V_{accAg} is the gas volume in accumulator A and n_{accA} is the polytropic exponent for accumulator A. Eq. 28 is substituted into Eq. 27 and rearranged as shown in Eq. 29.

$$\dot{p}_A = \frac{\beta}{V_A} \cdot \frac{(Q_{outp} - Q_{inm})}{1 + \frac{\beta \cdot V_{accAg}}{V_A \cdot n_{accA} \cdot p_A}} \tag{29}$$

3 WINCH CONTROL SYSTEM

In conventional swash plate units, the displacement is controlled by changing the angle of the swash plate. In digital hydraulic units, each piston has to be controlled individually resulting in an untraditional and complex control system. Section 2.2.2 and 2.2.3 describes the actuation sequence for the on/off valves when the piston runs in motor and pump mode respectively. This section describes how to decide which mode the pistons shall run in. Recall that θ_{mcm} shown in Fig. 5 describes the angle where the decision for motor mode is taken, and that θ_{mcp} shown in Fig. 6 describes the angle where the decision for pump mode is taken.

The control system for the winch is divided in two, one for the pump and one for the motor. In general, the motor has an open loop torque controller which calculates the displacement based on load measurements and a desired pressure drop across the motor. The pump has a displacement controller where the displacement is calculated based on the winch drum reference position and the known motor displacement. The pump also has a position feedback controller.

3.1 Motor Controller

The DHM is a radial piston motor with 42 cylinders. To ensure relatively smooth output torque, the motor is divided into 14 banks with three pistons in each bank that are evenly distributed around the shaft. Figure 7 illustrates the motor controller. Based on a desired pressure drop across the motor, Δp_{ref}, and measurements of the load, $\widetilde{M}_{Load}$. The number of active banks, also called n_{step}, is calculated a shown in Eq. 30.

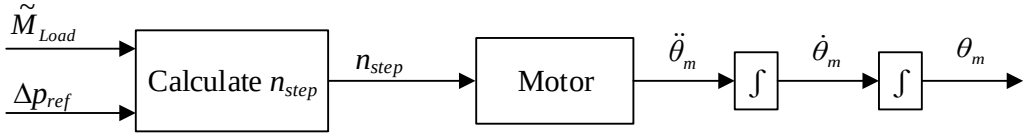

Figure 7: Motor controller

$$n_{step} \approx \frac{\widetilde{M}_{Load} \cdot g \cdot r_{winch}}{\Delta p_{ref} \cdot T_{step}}, \quad \text{round of to nearest integer} \tag{30}$$

where $n_{step} = 1$ corresponds to 1 active bank, $n_{step} = 2$ corresponds to 2 active banks and so on. T_{step} is the the torque one bank can provide with a pressure drop across the motor equal to 1 Pa.

3.2 Pump Controller

The controller for the DHP is based on the displacement controller first introduced in [3]. This controller is mainly used in digital hydraulic power management systems, but can also be used in DHPs. The controller calculates a desired volume, V_{des}, which the DHP shall deliver. If the desired volume is more than a half piston displacement higher than the volume the DHP already have delivered, V_{est}, the next piston will run in pump mode. If the difference is less than a half piston displacement, the next piston will run in idle mode. Figure 8 shows an example of the control strategy.

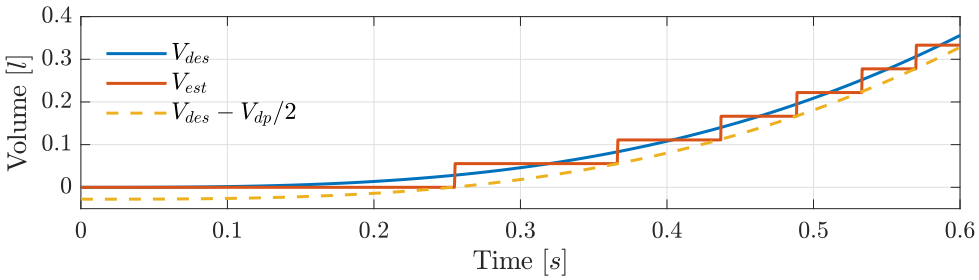

Figure 8: Example control strategy

In the control system used in this study, the desired volume consists of three different parts, V_{ref}, V_{accA} and V_{err}. Figure 9 illustrate the DHP controller where the mode choice, D, is calculated by Eq. 31.

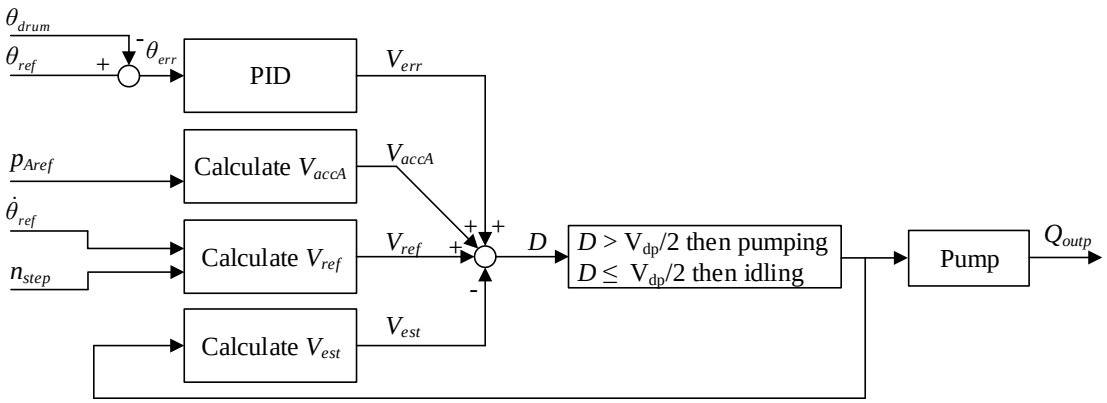

Figure 9: Pump controller

$$D = V_{ref} + V_{accA} + V_{err} - V_{est}, \quad \rightarrow \quad \begin{cases} \text{pumping} & \text{if} \quad D > V_{dp}/2 \\ \text{idling} & \text{if} \quad D \leq V_{dp}/2 \end{cases} \tag{31}$$

where V_{ref} is the estimated volume that is needed to drive the DHM according to the winch drum reference position and is calculated by integrating Eq. 32

$$\dot{V}_{ref} = \frac{V_{dm} \cdot n_{step} \cdot 3 \cdot \dot{\theta}_{ref}}{2 \cdot \pi} \tag{32}$$

where $\dot{\theta}_{ref}$ is the velocity reference of the winch drum.

The DHM is running with constant displacement. In order to accelerate or decelerate the payload, the pressure in line A has to be increased or decreased. When changing the pressure in line A, the fluid volume of accumulator A will also change. The estimated change of fluid volume in accumulator A, V_{accA}, is also included in the controller. V_{accA} is calculated as shown in Eq. 33.

$$V_{accA} = \frac{(p_{Aref} - p_{A0}) \cdot V_{accAg0}}{n_{accA} \cdot p_{A0}} \tag{33}$$

where p_{A0} is the initial pressure in line A, V_{accAg0} is the gas volume in accumulator A at the initial pressure p_{A0}, and p_{Aref} is the reference pressure in line A. p_{Aref} is calculated as shown in Eq. 34

$$p_{Aref} = \frac{\ddot{\theta}_{ref} \cdot J_{eff} + \widetilde{M}_{Load} \cdot g \cdot r_{winch}}{T_{step} \cdot n_{step}} + p_{B0} \tag{34}$$

where $\ddot{\theta}_{ref}$ is the acceleration reference for the winch drum and p_{B0} is the initial pressure in line B. The output, V_{err}, is calculated as shown in Eq. 35.

$$V_{err} = \theta_{err} \cdot k_p + \dot{\theta}_{err} \cdot k_d + \int \theta_{err} \cdot k_i \; dt \tag{35}$$

where θ_{err} is the difference between the reference winch drum position and the actual position and k_p, k_d and k_i are the PID-controller gains.

Finally, the estimated discharge volume, V_{est}, is calculated by the following equation.

$$V_{est} = n_{pump} \cdot V_{dp} \tag{36}$$

where n_{pump} is the total number of pistons that already have been pumping. The compression volume is not taken into account in Eq. 36 but can be included. In this control system, the small error introduced by excluding the compression volume will be compensated for in the PID-controller.

4 Simulation results

This section presents the simulation results. In all, six different cases are simulated. For a winch, it is obviously important to be able to hoist and lower a payload. These properties are shown in the first two sections. Because of the nature of DHPs and DHMs, the output flow or output torque can be pulsating, especially when running with very low displacements. Therefore the third section presents results where a light payload is hoisted with a very low velocity. Experience from the industry shows that it is hard to control very light payloads. The fourth section presents, therefore, simulation results of hoisting an empty hook. In the fifth section, an error in measurements of the payload is introduced to investigate the robustness of the controller. Normally, the same motor displacement can be used during short lifting operations, but for longer lifting operations it can be appropriate to change displacement due to changes in the load acting on the winch drum. The load acting on the winch drum can for example change when lifting a payload into or out of the water. In the last section, the simulation results show the effect of changing motor displacement while hoisting a constant load. In all cases, the feedback controller gains are the same and equal to $k_p = 0.1\ m^3$, $k_d = 0.025\ m^3 s$ and $k_i = 0.2\ m^3/s$.

4.1 Hoisting

This section presents the results of hoisting a payload equal to 18000 kg a distance of 10 m. The payload velocity is ramped up to 1 m/s with a ramp time of 2 s. Figure 10 shows the simulation results. The initial pressure in line B is 25 bar, and the desired pressure drop across the motor is 225 bar. The calculated motor step is $n_{step} = 13$.

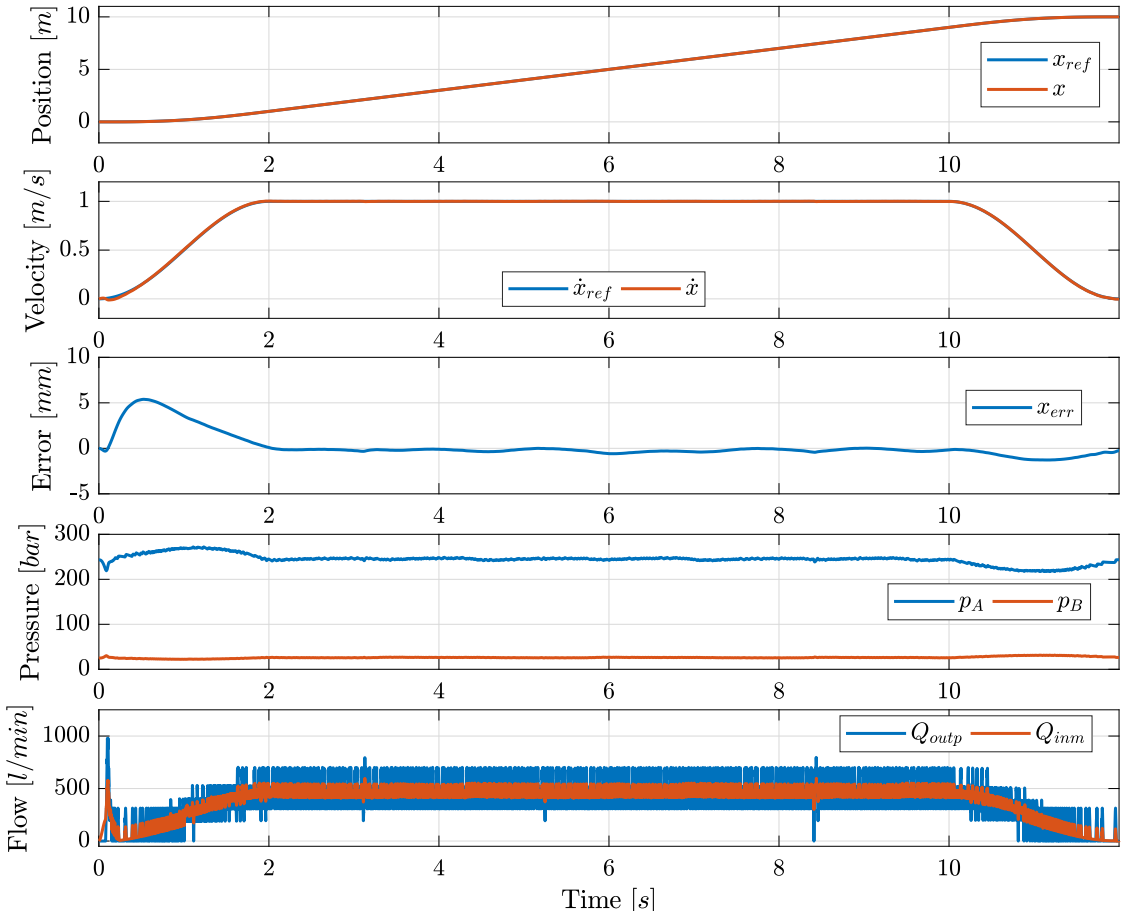

Figure 10: Simulation results of hoisting with $M_{Load} = 18000\ kg$, $\Delta p_{ref} = 225\ bar$, $p_{B0} = 25\ bar$, $k_p = 0.1\ m^3$, $k_d = 0.025\ m^3 s$, and $k_i = 0.2\ m^3/s$

The first and second plot show that the payload follows the position reference and the velocity reference well. The third plot shows that maximum position error occurs when accelerating the load and is approximately 5 mm. When the winch runs with constant speed, the position error is close to 0 mm. The fifth plot shows a flow peak in the beginning of the motion. This flow peak is needed to increase the pressure in line A and thereby increase the pressure drop across the motor and then accelerate the motor. The pump flow and motor flow are also heavily oscillating due to the concept of DHPs and DHMs. The pistons in DHPs and DHMs are enabled and disabled on a stroke by stroke basis resulting in flow and pressure ripples.

4.2 Lowering

This section presents the results of lowering a payload equal to 18000 kg a distance of 10 m. The velocity of the load is ramped down to -1 m/s with a ramp time of 2 s. Figure

11 shows the simulation results. When lowering the load, the DHP acts like a motor and the DHM acts like a pump, meaning that cylinders in the DHP can only run in motor or idle mode and the pistons in the DHM can only run in pump or idle mode. The same control strategy as described in Section 3 is used for both the DHP and the DHM. The initial pressure in line B is 25 bar and the desired pressure drop across the motor is 225 bar. The calculated motor step is $n_{step} = 13$.

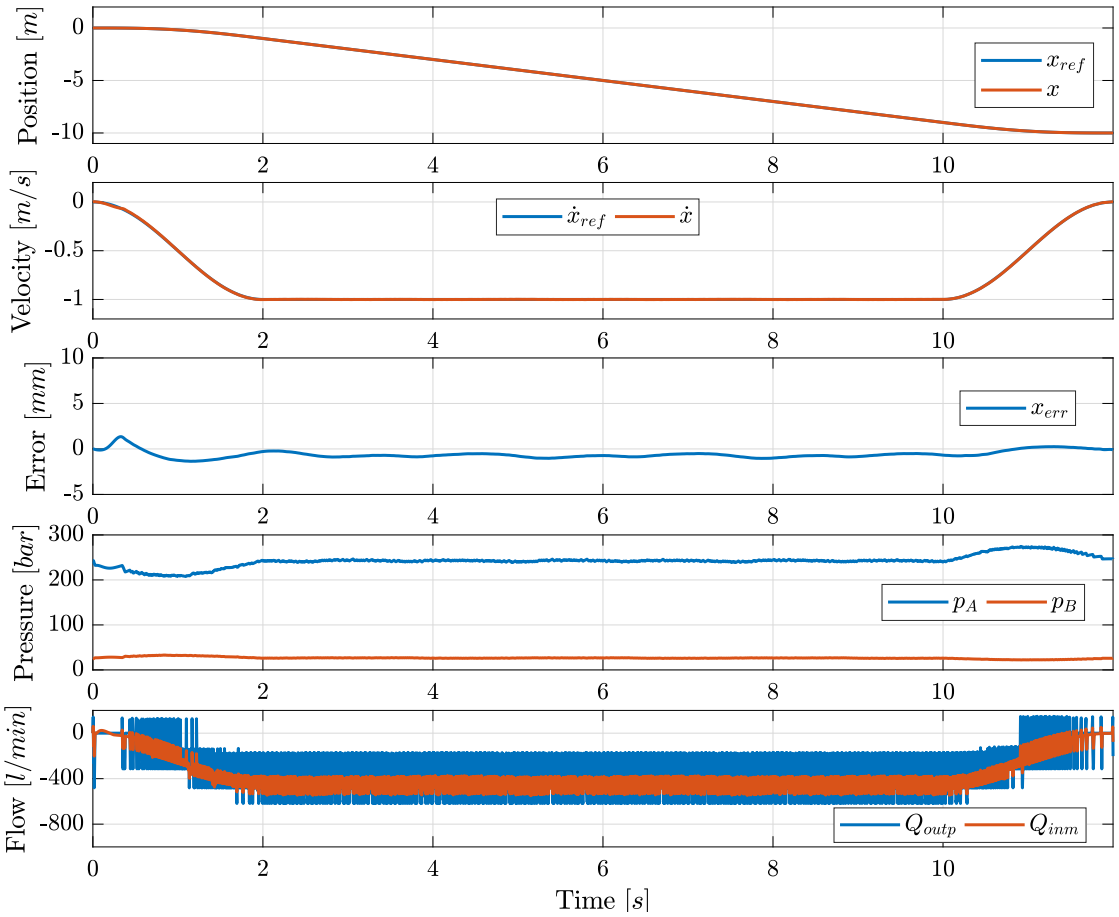

Figure 11: Simulation results of lowering with $M_{Load} = 18000\ kg$, $\Delta p_{ref} = 225\ bar$, $p_{B0} = 25\ bar$, $k_p = 0.1\ m^3$, $k_d = 0.025\ m^3 s$, and $k_i = 0.2\ m^3/s$

The simulation results show that the payload follows the reference position and velocity well. Maximum position error is smaller than 1.5 mm.

4.3 Hoisting Small Load at Low Speed

Every single cylinder in the DHP is controlled individually on a stroke by stroke basis, which results in flow ripples when running in partial displacement. In the closed circuit system studied in this paper, two accumulators are connected to pressure line A and pressure line B to smooth out flow and pressure ripples. One critical scenario is when the required pump flow is low. This scenario occurs when the velocity reference and the load is low. Therefore, in this test, the payload is set to 4000 kg and maximum velocity is set to 0.2 m/s. The payload is hoisted 5 m and the ramp time for the velocity is 2 s. Figure 12 shows the results with the initial pressure in line B equal to 25 bar and the desired pressure drop across the motor equal to 225 bar. The calculated motor step is $n_{step} = 3$.

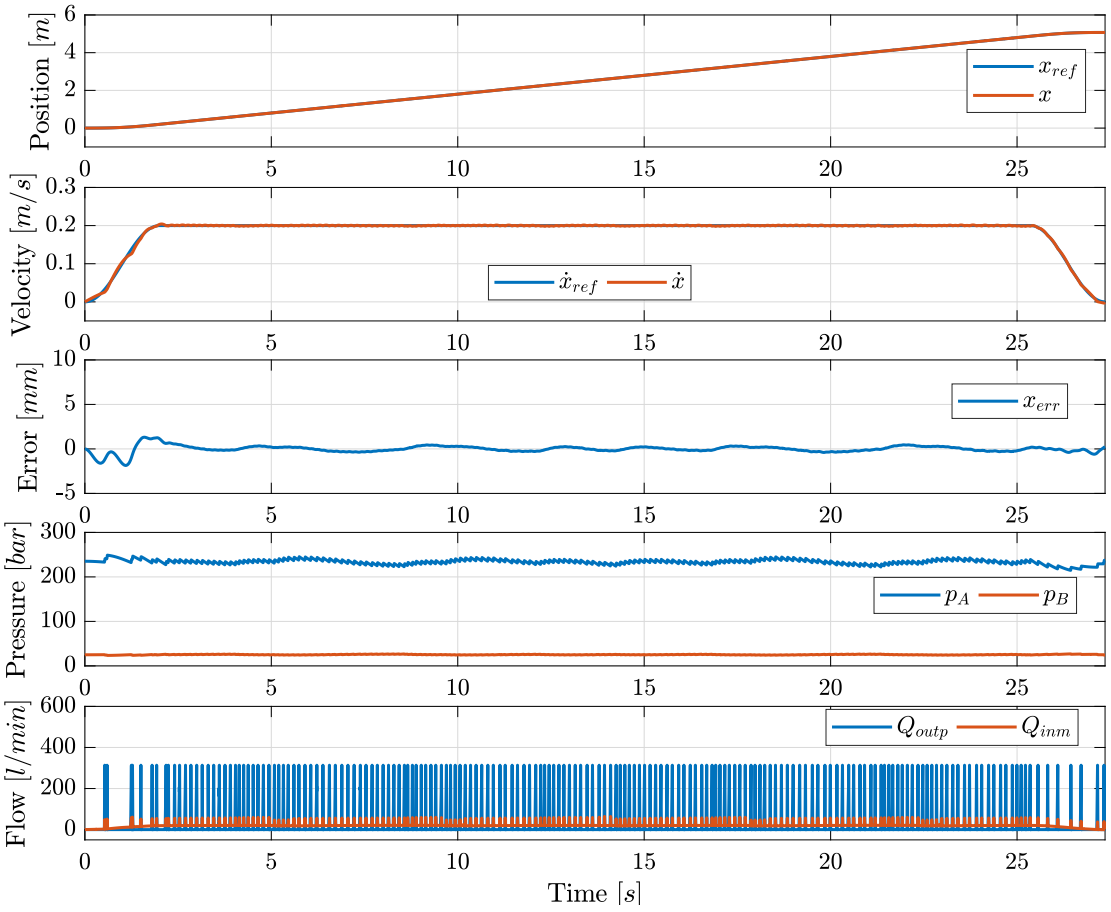

Figure 12: Simulation results of hoisting with $V_{max} = 0.2\ m/s$, $M_{Load} = 4000\ kg$, $\Delta p_{ref} = 225\ bar$, $p_{B0} = 25\ bar$, $k_p = 0.1\ m^3$, $k_d = 0.025\ m^3 s$, and $k_i = 0.2\ m^3/s$

The simulation results do not show any oscillations in velocity. The payload follows the position reference well with a maximum position error less than 2 *mm* when accelerating the load. The position error is close to 0 *mm* when the winch runs with constant speed. The simulated pump flow shows that the pump is only using one cylinder at a time. The average frequency of pumping cylinders is only 7 hz.

4.4 Hoisting an Empty Hook

This case tests driving with a payload equal to 0 *kg*, which corresponds to operating with an empty hook. The desired pressure drop across the motor is 0 *bar*. The empty hook is hoisted 10 *m* and the velocity is ramped up to 1.5 m/s with a ramp time of 3 *s*. Because of the low pressure drop across the motor and the high inertia of the winch drum and the wire, the initial pressure in line *B* is set to 125 *bar* and the motor step is set to $n_{step} = 3$ to ensure that the pressure in line *A* remains above the minimum pressure for accumulator *A* while decelerating the load.

The simulation results show that the payload follows the reference position and velocity well. The maximum position error is approximately 3.5 *mm* and occurs right after the payload reaches maximum velocity. The position error converges towards 0 *mm* when the winch drum runs with constant velocity.

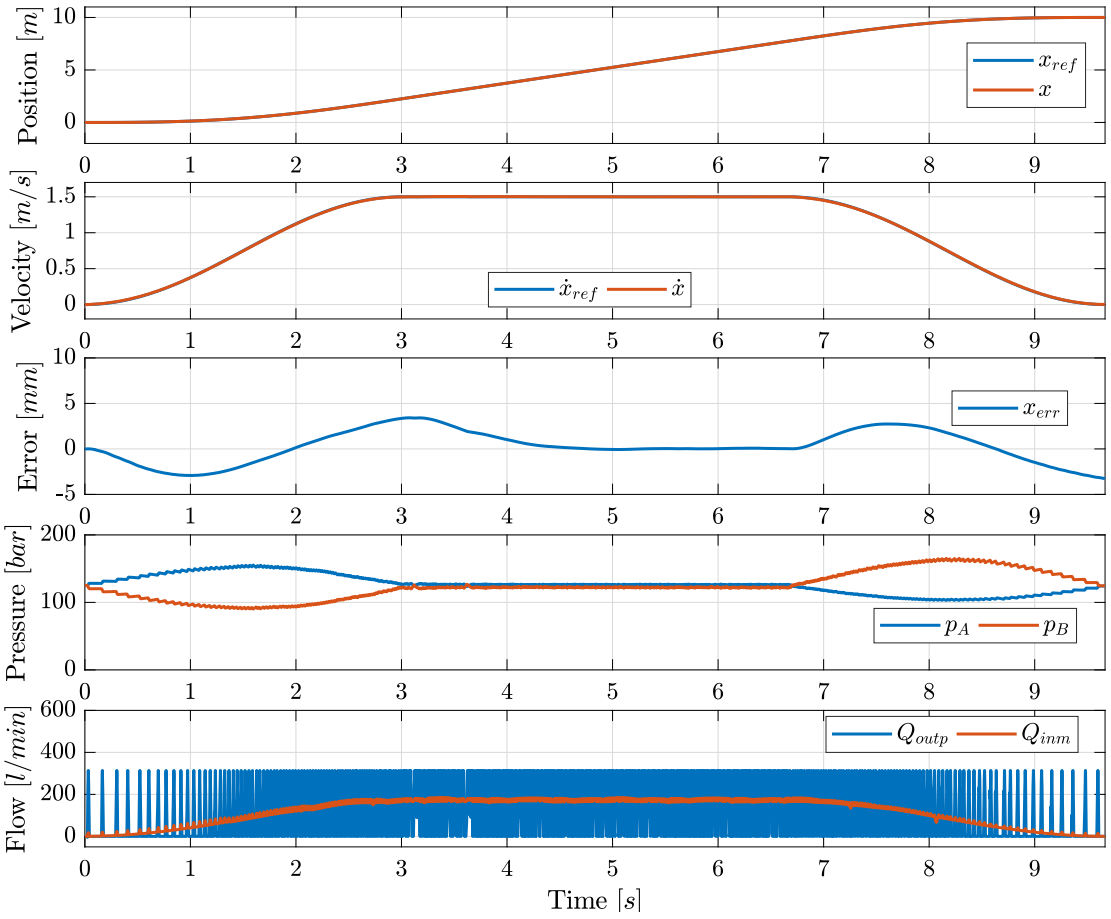

Figure 13: Simulation results of hoisting with $M_{Load} = 0kg$, $\Delta p_{ref} = 0bar$, $p_{B0} = 125\ bar$, $k_p = 0.1\ m^3$, $k_d = 0.025\ m^3 s$, and $k_i = 0.2\ m^3/s$

4.5 Error in Load Measurement

Motor displacement is calculated based on a desired pressure drop across the motor and measurements of the payload. In this test, an error in the payload measurements is introduced to investigate the robustness of the control system. The actual payload is set to 18000 kg, but the measured value used in the controller is only 80 % af the actual load. The payload is hoisted 10 m and the velocity is ramped up to 1 m/s with a ramp time of 2 s. The simulation results are shown in Fig. 14. The initial pressure in line B is set to 25 bar and the desired pressure drop across the motor is 225 bar. The calculated motor step is $n_{step} = 11$.

This case is similar to the case presented in Section 4.1 except for the error in the load measurements. The simulation results show that an error in the payload measurements gives almost the same results as in Section 4.1. The maximum position error is increased to 7.4 mm. Due to the measurement error, the calculated motor displacement is only $n_{step} = 11$ compared to $n_{step} = 13$ for the case without any measurements error. The difference in motor displacement results in a higher pressure in line A and a lower pump flow, but the position tracking performance remains almost unchanged.

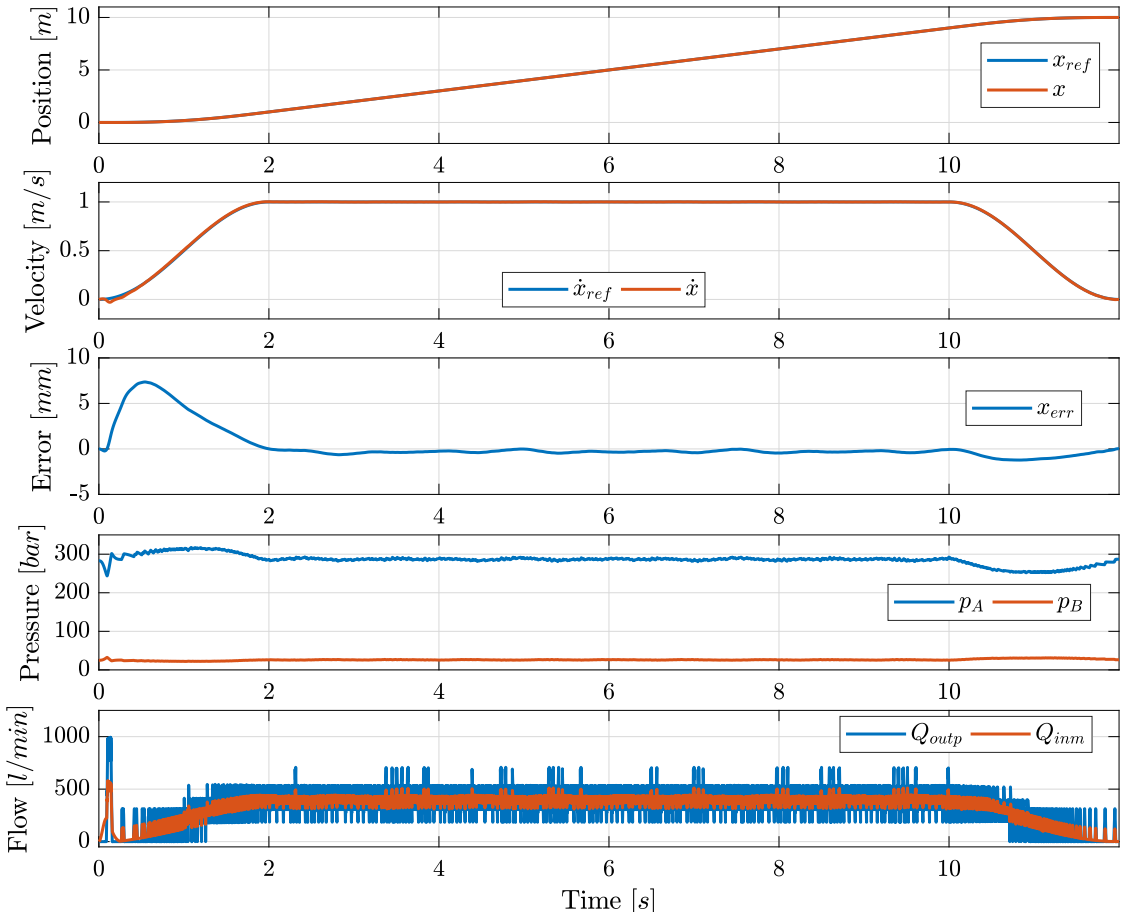

Figure 14: Simulation results of hoisting a load with measured load equal 80 % of the real load and where $M_{Load} = 18000\ kg$, $\Delta p_{ref} = 225\ bar$, $p_{B0} = 25\ bar$, $k_p = 0.1\ m^3$, $k_d = 0.025\ m^3 s$, and $k_i = 0.2\ m^3/s$

4.6 Change of Motor Displacement

The winch studied in this paper has a capacity of 3600 m of wire. In cases where the load is lifted or lowered several hundreds of meters, the load acting on the winch drum will vary. The load can vary because the weight of the wire will act as an extra load when lowering or because the load is lowered into water. In cases like this, the motor must be able to change displacement during operation. Figure 15 shows results from hoisting of a constant load equal to 15000 kg with a change in motor step from $n_{step} = 11$ to $n_{step} = 14$, full displacement, after 4 s. The initial pressure in line B is 25 bar and the desired pressure drop across the motor is 225 bar.

The motor starts to change displacement after 4 s. The time it takes to change motor displacement is dependent of the motor speed. The motor have to rotate more than a half shaft revolution, $(2 \cdot \pi - \theta_{mcm} + \pi)$, to fully change displacement. When hoisting the payload with 1 m/s, the motor response time is approximately 4.4 s.

When changing motor displacement the position error increases to -3 mm, but approximates zero when the motor displacement has reached full displacement. In the pressure plot, it can be seen that the pressure in line A decreases when the motor displacement is changed. It can also been seen that the pump flow and motor flow increase.

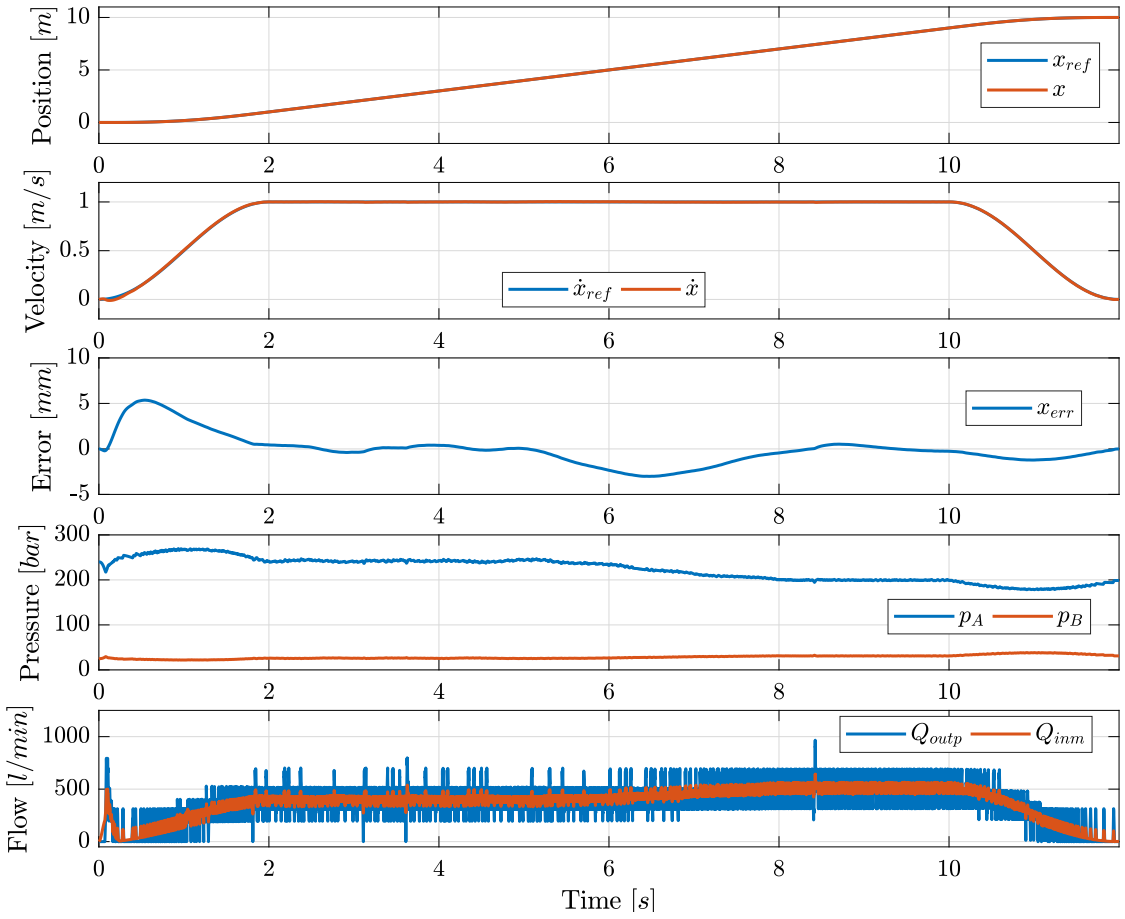

Figure 15: Simulation results of hoisting a load when changing motor step from step 11 to step 14 with $M_{Load} = 15000\ kg$, $\Delta p_{ref} = 225\ bar$, $p_{B0} = 25\ bar$, $k_p = 0.1\ m^3$, $k_d = 0.025\ m^3 s$, and $k_i = 0.2\ m^3/s$

5 CONCLUSION

This simulation study investigates the feasibility of using a digital hydraulic winch drive system on a 20000 *kg* hydraulic offshore auxiliary winch. Hoisting and lowering a payload equal to 18000 *kg* have been investigated in addition to handling low load at low speed, no load at high speed, error in load measurements and change of motor displacement while operating.

The simulation results show that DHPs and DHMs have the potential of driving a winch with high precision and controllability in a wide range speeds and loads. The highest position error was 7.4 *mm* and occurred when an error in the measured load was introduced. Even though the output flow of the DHP at partial displacement pulsates, the velocity of the payload was smooth in all the tested cases.

The same controller and control parameters were used for all simulation cases. An error in the load measurements was introduced to investigate the robustness of the controller. The simulated results show that the error in load measurement did not introduce significant changes in controllability of the winch.

References

[1] M. Umaya, T. Noguchi, M. Uchida, M. Shibata, Y. Kawai, and R. Notomi, "Wind power generation - development status of offshore wind turbines," *Mitsubishi Heavy Industries Technical Review*, vol. 50, pp. 29–35, September 2013.

[2] E. de Vries, "Mitsubishi launches 7*MW* turbine," Januar 2012. URL `http://www.windpowermonthly.com/article/1109873/mitsubishi-launches-7mw-turbine`.

[3] M. Heikkilä and M. Linjama, "Direct connection of digital hydraulic power management system and double acting cylinder-a simulation study," *The Fourth Workshop on Digital Fluid Power, Linz, Austria*, September 2011.